Chemical Science

ROYAL SOCIETY OF CHEMISTRY

EDGE ARTICLE

View Article Online
View Journal | View Issue

Cite this: *Chem. Sci.*, 2024, **15**, 17210

All publication charges for this article have been paid for by the Royal Society of Chemistry

Received 14th June 2024
Accepted 16th September 2024

DOI: 10.1039/d4sc03907f

rsc.li/chemical-science

Visible light-induced Mallory reaction of tertiary benzanilides *via* iminium intermediates†

Xiaoqiang Ma,‡ Si Wang,‡ Zhanyong Tang, Jialin Huang, Tianhao Jia, Xingda Zhao and Depeng Zhao *

The Mallory reaction, which involves the photocyclization of stilbenes/diarylethenes and their analogues into polycyclic aromatics, is of significant synthetic importance. However, its application to tertiary benzanilides has not been explored to date. Besides, most of the reported Mallory reactions require ultraviolet irradiation. In this study, we show the first Mallory reaction of tertiary benzanilides promoted by visible light *via* iminium intermediates formed *in situ* from tertiary benzanilide, Tf_2O (triflic anhydride) and pyridine. UV/vis absorption spectroscopy combined with density functional theory (DFT) calculations revealed that the formation of the iminium intermediate decreased the HOMO–LUMO energy gap, thereby enhancing visible light absorption. This study provides a rapid and practical approach for the preparation of the phenanthridinone skeleton and provides a new idea for the design of new visible light photoswitches.

Introduction

Since its discovery in 1964,[1,2] the Mallory reaction has become a powerful synthetic tool for the construction of polycyclic aromatic hydrocarbons and heterocyclic analogues, from simple phenanthrenes and their heterocyclic analogues to complex polycyclic molecules (coronenes, helicenes, *etc.*) and nanographenes/graphene nanoribbons.[3–9] The typical examples of Mallory reactions are shown in Fig. 1B. Under UV irradiation, stilbene or its derivatives undergo 6π-electrocyclization and further oxidation or elimination, resulting in the formation of phenanthrene derivatives.[10–12] Though the Mallory-type reaction of benzamides (ArCONHAr) was first reported as early as 1967,[13–16] the Mallory-type reaction of tertiary benzanilides remains undeveloped with no clear reason given thus far (Fig. 1B).

Phenanthridinone skeletons are important subunits found extensively in natural products and pharmaceutical compounds (Fig. 1A).[17–23] For example, they have been widely used as the PARP inhibitor for anticancer therapies and as neurotrophin activity enhancers for the treatment of nerve diseases.[24–28] Over the past several decades, many approaches with the pre-functionalization of the aryl groups of tertiary benzanilides have been developed.[20,29–36] Recently, two fascinating examples of C–C cross-coupling reactions involving benzanilides with two unactivated sp^2 hybridized C–H bonds were reported (Fig. 1C).[37] However, in the first example of Pd-catalysed intramolecular oxidative *ortho*-arylation of benzanilides, the substrate scope is limited and, in particular, halogens are incompatible. In the latter case of electrochemical intramolecular cross-coupling,[38] the scope of the benzoyl moiety is strictly limited to electron-rich aryls with two or more alkoxy groups (Fig. 1C). Given such significance, the development of concise and versatile methods to obtain these high-value skeletons remains a topic of general interest.

Although previous studies,[39] including our NMR results, indicate that the *N*-methylbenzanilide mainly exists in *cis*-conformation which should facilitate its photocyclization, attempts to induce its photocyclization under UV light have remained unsuccessful. We inferred that the observed phenomena can be attributed to the resonance of tertiary benzanilides. Although tertiary benzanilide can be described as a resonance between neutral and zwitterionic forms,[40,41] the zwitterionic form (which is a good 6π system) makes less contribution to the whole structure (Fig. 1D), resulting in poor photocyclization upon light irradiation. We reasoned that increasing the C=N double bond character would enhance the feasibility of 6π photocyclization. As tertiary benzanilides are known to form the oxyiminium ion upon treating with Tf_2O, our initial study focused on the Tf_2O-mediated[42] photocyclization of *N*-methylbenzanilide. To our delight, the desired product **2a** was obtained in 60% ^1H NMR yield under 310 nm UV light (see ESI† page 14 for more details). Notably, due to the wide band gaps between the valence and conduction bands, Mallory-type reactions are constrained by their reliance on photoactivity primarily within the UV region.[43–45] Based on the previous

State Key Laboratory of Anti-infective Drug Discovery and Development, School of Pharmaceutical Sciences, Sun Yat-sen University, Guangzhou, 510006, China. E-mail: zhaodp5@mail.sysu.edu.cn

† Electronic supplementary information (ESI) available. See DOI: https://doi.org/10.1039/d4sc03907f

‡ These authors made equal contributions to this work.

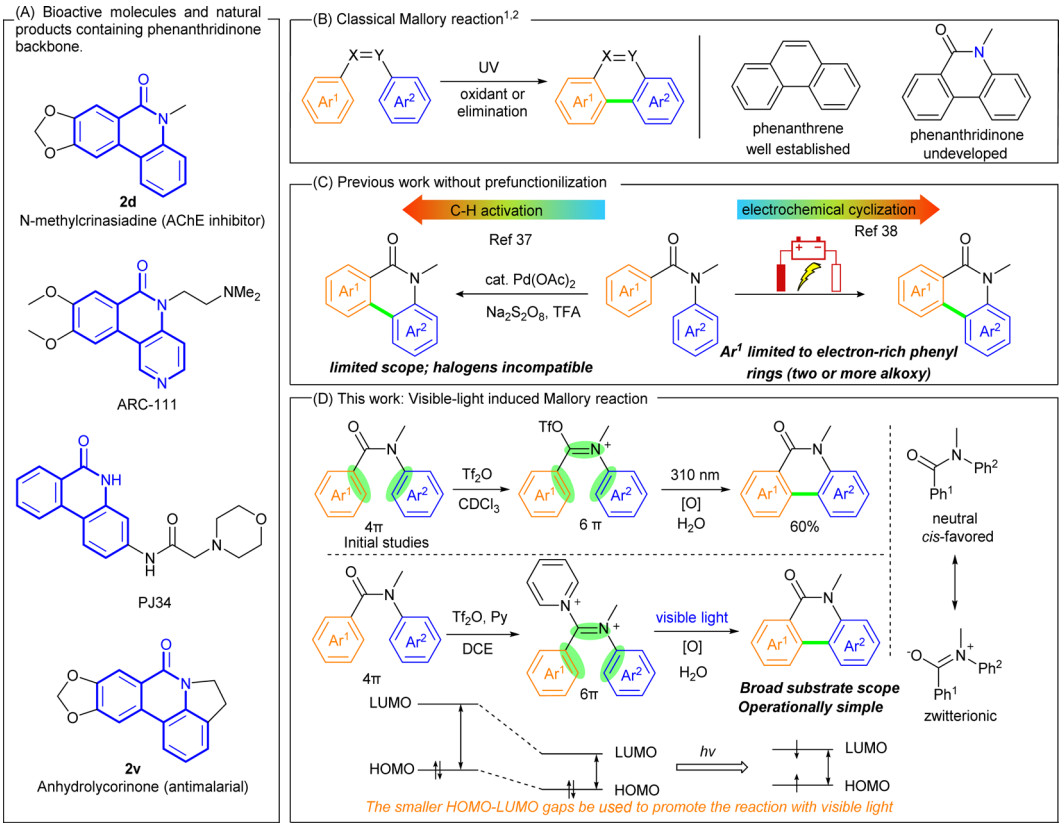

Fig. 1 Background and design for the visible light-promoted cyclization.

reports from our group[46,47] and others on iminium salts[48–52] in photochemical reactions, we planned to investigate the photochemical reactivities of iminium salts of tertiary benzanilide promoted by visible light. We were delighted to find that the iminium intermediate formed *in situ* from *N*-methylbenzanilide **1a**, Tf_2O and Py (pyridine) exhibited a yellow colour, indicating its absorption of visible light. We hypothesized that the iminium intermediate might undergo a 6π cyclization under visible light as a result of the small energy gap between the highest occupied molecular orbital (HOMO) and lowest unoccupied molecular orbital (LUMO), resulting in the formation of **2a** upon oxidative aromatization. Herein, we demonstrate the first Mallory-type reaction of tertiary benzanilide to construct phenanthridinone scaffolds *via* iminium intermediates triggered by visible light. This protocol was successfully applied to the concise total synthesis of a natural alkaloid anhydrolycorinone **2v** and an AChE inhibitor *N*-methylcrinasiadine **2d**.[53,54] Density functional theory (DFT) calculation studies revealed that a difference in the delocalization contributes to the decrease in the HOMO–LUMO energy gap of the iminium formed *in situ*.

Results and discussion

We commenced our investigation by irradiating *N*-methylbenzanilide **1a** in 1,2-dichloroethane (DCE) at 25 °C with 425 nm blue light in the presence of Tf_2O (2.0 equiv.) and pyridine (2.0 equiv.) for 20 h. We were pleased to find that the

Table 1 Optimization of the reaction conditions[a]

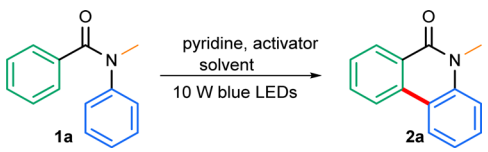

Entry	Pyridine (equiv.)	Activator (equiv.)	Solvent	Yield[b] (%)
1	Pyridine (1.6)	Tf_2O (1.1)	DCE	27
2	Pyridine (2.0)	Tf_2O (2.0)	DCE	40
3	Pyridine (3.0)	Tf_2O (3.0)	DCE	65
4	Pyridine (3.0)	Tf_2O (2.0)	DCE	90[c]
5	Pyridine (3.0)	TfOH (2.0)	DCE	NR
6	Pyridine (3.0)	$SOCl_2$ (3.0)	DCE	NR
7	Pyridine (3.0)	$(COCl_2)$ (2.0)	DCE	NR
8	2-Acetylpyridine (3.0)	Tf_2O (2.0)	DCE	NR
9	4-Methoxypyridine (3.0)	Tf_2O (2.0)	DCE	NR
10	2-Methylpyridine (3.0)	Tf_2O (2.0)	DCE	25
11	Pyridine (3.0)	Tf_2O (2.0)	DCM	80
12	Pyridine (3.0)	Tf_2O (2.0)	EA	34
13	Pyridine (3.0)	Tf_2O (2.0)	MeCN	69
14	Pyridine (3.0)	—	DCE	NR
15	—	Tf_2O (2.0)	DCE	NR
16[d]	Pyridine (3.0)	Tf_2O (2.0)	DCE	NR
17[e]	Pyridine (3.0)	Tf_2O (2.0)	DCE	84

[a] Unless otherwise mentioned, all reactions were conducted with **1a** (0.2 mmol), solvent (2.0 mL), 25 °C, N_2, 10 W blue LEDs, 20 h. [b] Isolated yield. [c] Identical yield was observed for 12 h. [d] Under dark. [e] Without an inert gas atmosphere. 1,2-Dichloroethane (DCE), dichloromethane (DCM), acetonitrile (MeCN), ethyl acetate (EA).

desired phenanthridinone product **2a** was indeed obtained in 40% yield (Table 1, entry 2). With these preliminary results in hand, we then systematically screened the reaction conditions to improve the yield. A notable enhancement was observed employing 3.0 equiv. of Tf_2O and pyridine, resulting in an increase in the yield to 65% (entry 3). To our delight, on using 3.0 equiv. pyridine with 2.0 equiv. Tf_2O, the yield increased significantly from 65% to 90% (entry 4). Apart from Tf_2O, no desired product was detected when other activators such as trifluoromethanesulfonic acid (entry 5), thionyl chloride (entry 6) or oxalyl chloride (entry 7) were used. Other substituted pyridines were also tested; however, 2-acetylpyridine (entry 8) and 4-methoxypyridine (entry 9) failed to yield the product, and 2-methylpyridine (entry 10) provided **2a** in a low yield (25%). Therefore, we chose 2.0 equiv. of Tf_2O and 3.0 equiv. of pyridine for further investigations of commonly used solvents, such as dichloromethane (DCM), ethyl acetate (EA), and acetonitrile (CH_3CN). However, none of the above solvents could provide higher yields than that of DCE (entries 11–13). Finally, control experiments confirmed that light, Tf_2O and pyridine are all essential for this transformation. No product was observed in the absence of these reaction components (entries 14–16). It is worth noting that this reaction also proceeds without an inert gas atmosphere with a slight decrease in yield (84%, entry 17). Unfortunately, reducing the equivalents of Tf_2O (1.1 equiv.) and

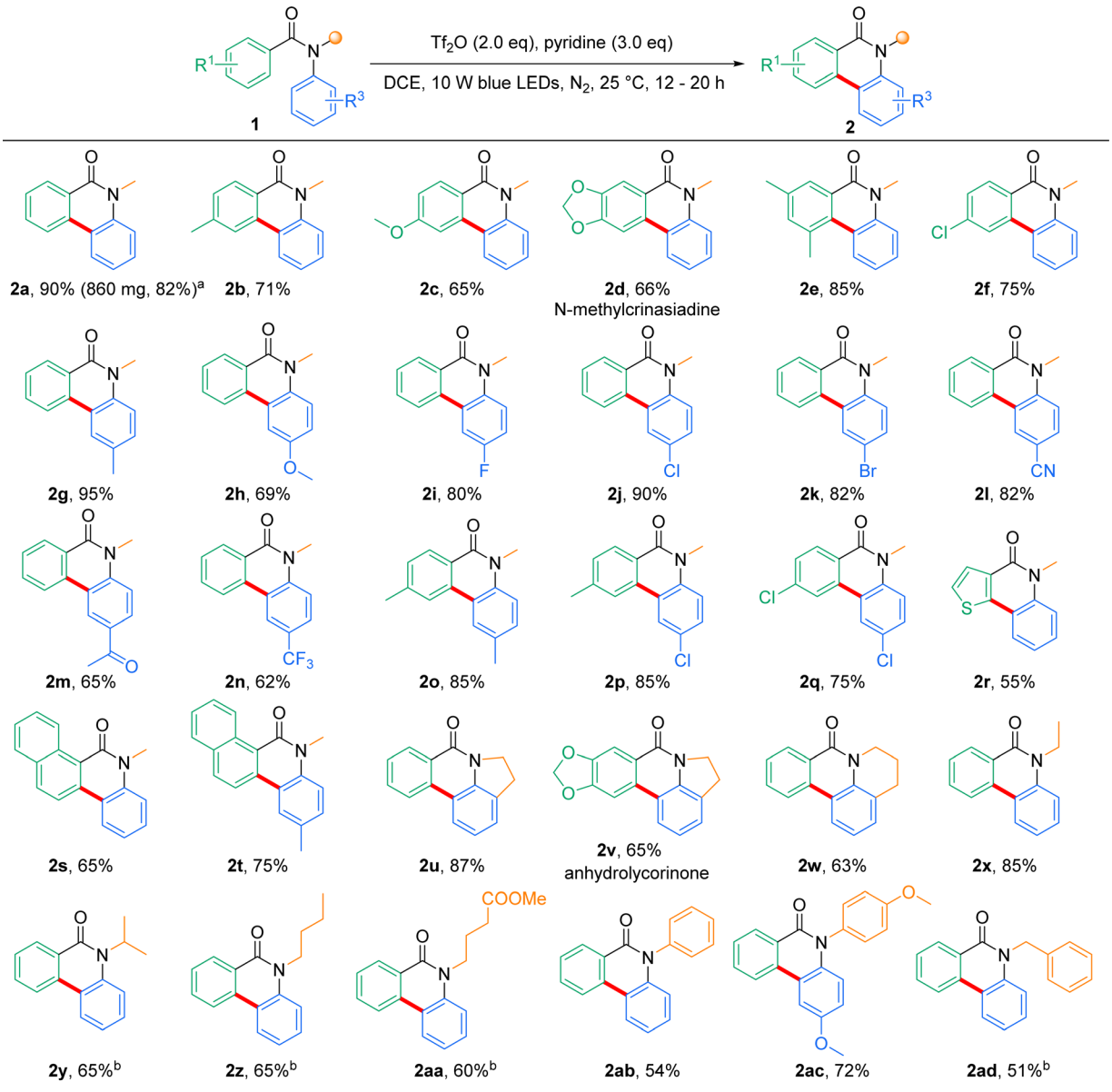

Scheme 1 Substrate scope of the photocyclization. Reaction conditions: **1** (0.2 mmol, 1.0 equiv.), Tf_2O (0.4 mmol, 2.0 equiv.), pyridine (0.6 mmol, 3.0 equiv.), DCE (2.0 mL), 25 °C, N_2, 10 W blue LEDs (425 nm), 12–20 h, yields of isolated product. [a]5.0 mmol scale, 36 h. [b]4.0 equiv. Tf_2O and 6.0 equiv. pyridine.

pyridine (1.6 equiv.) resulted in a considerably lower yield of **2a** (27%, entry 1).

With the optimal conditions established, the substrate scope was next explored to probe the generality of this reaction in the synthesis of phenanthridinone derivatives (Scheme 1). Initially, various electron-donating substitutions on the benzoyl derivatives were tested in the photocyclization reaction. When substrates with benzoyl derivatives bearing 4-methyl (**1b**), 4-methoxyl (**1c**), piperonyl (**1d**), and 3,5-dimethyl (**1e**) were subjected to the standard conditions, the cyclization products **2b**, **2c**, **2d** and **2e** were afforded in good to excellent yields (71%, 65%, 66%, and 85%, respectively). Substrate (**1f**) with an electron-withdrawing group (Cl) in the benzoyl moiety was suitable for this transformation, affording **2f** in a good yield (75%). Subsequently, substrates with methyl (**1g**), methoxyl (**1h**), halogens (**1i–1k**), cyano (**1l**), acetyl (**1m**) and trifluoromethyl (**1n**) with the aniline moiety were also examined, and moderate to excellent yields were observed (62–95%). Substrates containing fluorine or trifluoromethyl groups, which are commonly used in medicinal chemistry to enhance the lipophilicity, are suitable for this reaction (**2i** and **2n**).[55] To our delight, this iminium activation strategy was viable for both benzoyl and aniline-substituted *N*-methylbenzanilide, affording the annulation target **2o–2q** with satisfactory results (yields: 85%, 85% and 75%, respectively). It is evident that the presence of both electron-donating and electron-withdrawing groups on the *N*-methylbenzanilides does not considerably impact the reaction yield. Encouraged by the above results, we next tested our strategy of polycyclic or heterocyclic-substituted anilide derivatives (**1r–1t**). Specifically, **2s** and **2t** were obtained in relatively high yields (65% and 75%), whereas **2r** was obtained in 55% yield, which might be due to the instability of the thiophene moiety under the reaction conditions.

To further explore the generality of this photocyclization, we next examined the compatibility of *N*-substituents. When benzanilides bearing five- or six-membered cyclic amine moiety

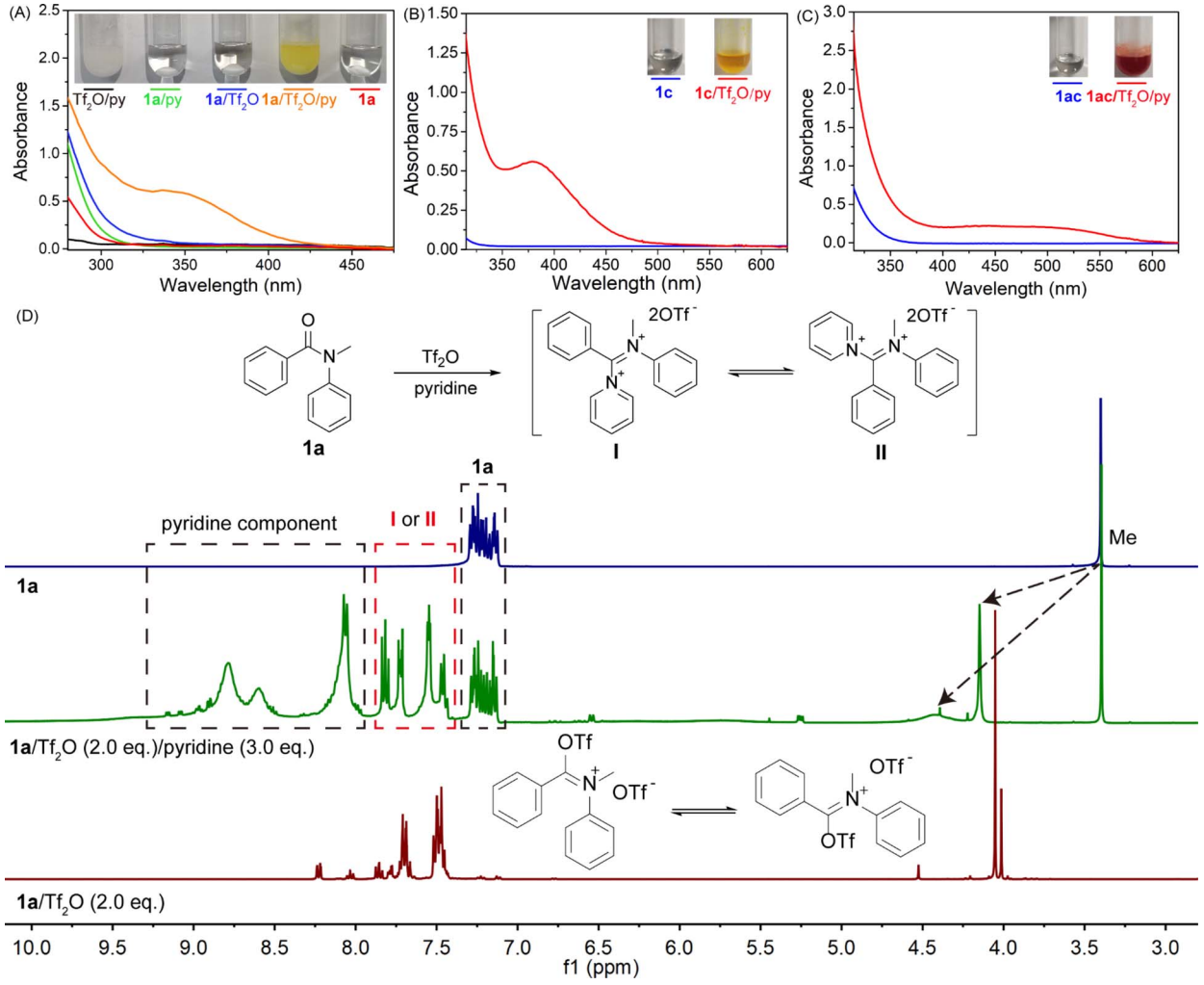

Fig. 2 UV/vis absorption spectra of (A) Tf_2O and pyridine; **1a** and pyridine (3.0 equiv.); **1a** and Tf_2O (2.0 equiv.); **1a**, Tf_2O (2.0 equiv.) and pyridine (3.0 equiv.); **1a** in DCE (5×10^{-5} mol L^{-1}); (B): **1c**; **1c**, Tf_2O (2.0 equiv.) and pyridine (3.0 equiv.) in DCE (5×10^{-5} mol L^{-1}); (C) **1ac**; **1ac**, Tf_2O (2.0 equiv.) and pyridine (2.0 equiv.) in DCE (5×10^{-5} mol L^{-1}); inset: colour changes of the corresponding substrate and mixture (5×10^{-3} mol L^{-1}); (D) ^1H NMR experiments: **1a** (0.05 mmol) in CD_3CN (0.5 mL); mixture of **1a** (0.05 mmol), Tf_2O (2.0 equiv.) and pyridine (3.0 equiv.) in CD_3CN (0.5 mL); mixture of **1a** (0.05 mmol) and Tf_2O (2.0 equiv.) in CD_3CN (0.5 mL).

were subjected to the standard reaction conditions, the corresponding polycyclic products (**2u–2w**) were afforded in moderate to high yields (87%, 65% and 63%, respectively). Likewise, the cyclization with benzanilides having linear aliphatic *N*-substitutions, such as ethyl (**1x**), ^{i}propyl (**1y**), ^{n}butyl (**1z**) and 4-butanoate (**1aa**), all furnished the corresponding products **2x–2aa** in moderate to high yields (85%, 65%, 65% and 60%, respectively), although 4.0 equiv. Tf_2O and 6.0 equiv. pyridine were required for **1y–1aa**. In addition, we evaluated the performance of *N*,*N*-diaryl substituted benzanilides; both **1ab** (phenyl) and **1ac** (4-methoxyphenyl) proved to be effective for this protocol, affording products **2ab** and **2ac** in good yields (54% and 72%). Finally, benzyl *N*-substituted substrate **1ad** also worked well under this protocol (51%), albeit with 4.0 equiv. Tf_2O and 6.0 equiv. pyridine. To explore the practical utility of this transformation in organic synthesis, a gram-scale experiment of **1a** (5.0 mmol, 1.05 g) was performed, which gave rise to a satisfactory yield of the cyclization product **2a** (0.86 g, 82%). Notably, many of the annulation products, such as **2d** and **2v**, are important subunits in biologically and pharmaceutically-active phenanthridinone alkaloids or their analogues.[53,54]

To probe the reaction mechanism and validate the involvement of visible light in the Mallory reaction process, we conducted UV/vis spectroscopy experiments. The UV/vis absorption spectra of **1a**, **1a**/Tf_2O/pyridine, **1a**/Tf_2O, **1a**/pyridine, and Tf_2O/pyridine are shown in Fig. 2A. As expected, a new absorption band at 360 nm appeared for the ternary mixture of **1a**/Tf_2O/pyridine with the tail absorption extending until 425 nm, indicating the formation of a new species (orange line, Fig. 2A). In contrast, all the reagents or binary mixtures exhibit weak absorption above 350 nm. Furthermore, Fig. 2A (inset) shows the solution colour contrast from colourless to light-yellow, indicating visible light absorption of the iminium intermediate. Note that other iminiums formed *in situ* from tertiary benzanilides (**1c**, **1k**, **1l**, **1s**, **1u** and **1ac**), Tf_2O and pyridine also exhibit visible absorbance bands (Fig. 2B, C and Fig. S4†). Additionally, to validate our strategy of iminium-induced visible light absorption, ^{1}H NMR spectroscopy studies were performed to confirm the formation of the iminium intermediate. As shown in Fig. 2D and S6,† when **1a** was treated with 2.0 equiv. Tf_2O and 3.0 equiv. pyridine in anhydrous CD_3CN. To our delight, two new peaks of *N*-methyl hydrogen were observed (4.15 and 4.43 ppm). Besides, in the aromatic region, four new sets of signals of the iminium intermediate were observed, indicating the formation of the iminium intermediate (7.40–7.85 ppm). To gain an insight into the reaction mechanism, gas chromatography (GC) was employed to analyse the gases in the Schlenk tube of the reaction of **1a** under standard conditions. The results indicated that hydrogen was generated during the reaction (see ESI† page 43 for more details). In addition, radical trapping experiments were performed (Fig. 4A). The presence of radical scavengers (TEMPO or BHT) did not drastically inhibit the formation of product **2a**, excluding the participation of radical species.

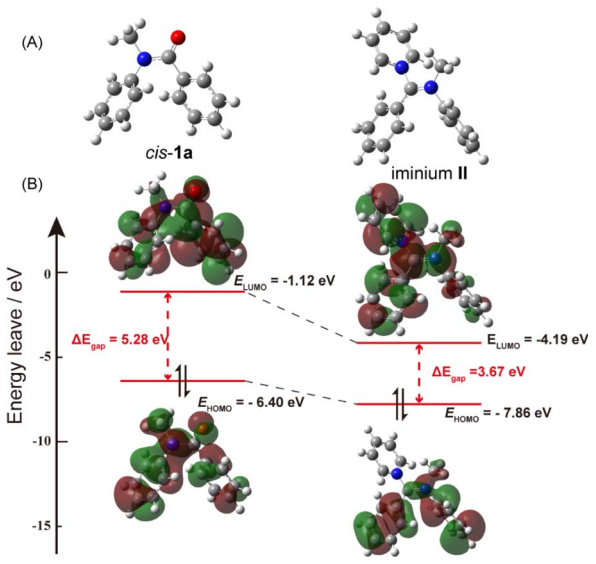

Fig. 3 (A) Optimized molecular structure of *cis*-**1a** and iminium intermediate **II**; (B) HOMO and LUMO orbital levels and energy gap of *cis*-**1a** and iminium intermediate **II**, calculated with DFT at the B3LYP-D3(BJ)/def2-TZVP level using Gaussian 16.

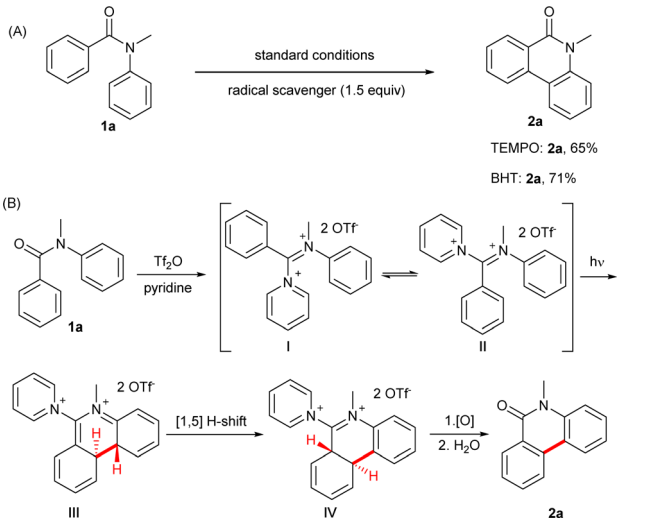

Fig. 4 (A) Radical trapping and (B) plausible reaction mechanism.

We further employed theoretical calculation to confirm that the formation of the iminium intermediate causes intramolecular cyclization under visible light irradiation (see Computational details in ESI†). The molecular minimized structure of **1a** and iminium **II** are shown in Fig. 3A and S1.† As previously reported, the calculated stilbenes correspond to the optimal *cis* conformation for the photocyclization reaction.[56] Fig. 3B shows the frontier molecular orbitals of the *cis* conformation of **1a** and iminium **II**, where red and green colours indicate two opposite phases of orbitals, *i.e.*, positive (or crest) and negative (or trough) regions of molecular orbitals, respectively. For single **1a**, both the HOMO and LUMO are spread over the entire molecule, as illustrated in Fig. 3B. However, in iminium **II**, the HOMO mainly concentrates on the phenyl and *N*-methylaniline, while the LUMO is located on the whole iminium **II**. The evaluated energies of the HOMO–LUMO energy

gap of **1a** and iminium intermediate **II** were found to be 5.28 and 3.67 eV, respectively. The observed decrease in the HOMO–LUMO energy gap can be attributed to differential delocalization, where LUMO shows a more significant reduction during the formation of iminium intermediates.[57,58] To analyse the spatial distribution of the electron–hole after iminium **II** excitation, the electron–hole excitation analysis of iminium **II** was performed using Multiwfn.[59,60] The results showed charge transfer (CT) excitation from the aniline (HOMO) to the pyridine moiety (LUMO). This charge transfer state may prolong the excited lifetime.[61–63] This small HOMO–LUMO energy gap accounts for the crucial electronic transitions decrease and the absorption wavelength shows the bathochromic effect. Furthermore, the $E_{0,0}$ of iminium **II** was also estimated from the wavelength at the intersection point of the normalized UV-vis absorption spectrum and the emission spectrum in solution (367 nm, 3.37 eV, Fig. S5†). Additionally, we speculate that intermolecular interactions might be responsible for the absorption at ~425 nm, as confirmed by the calculation of the HOMO–LUMO energy gap of the D–A complex **1a**/iminium **II** (Fig. S1†).

Based on the above results and previous work,[46,47,64] we proposed a plausible reaction mechanism (Fig. 4B). Firstly, iminium intermediate **I** was formed *in situ*.[50,65] Subsequently, iminium intermediate **I** was tautomerized into iminium intermediate **II**.[66,67] Followed by a photochemical 6π-electrocyclization under visible light conditions, iminium intermediate **III** was generated by ring closure. Then, intermediate **III** was expected to undergo a suprafacial [1,5]-H shift, affording intermediate **IV**, which is driven by the aromatization.[45,68,69] In the end, intermediate **IV** was converted to phenanthridinone *via* oxidation or dehydrogenation and hydrolysis.

Conclusions

In summary, we report the first Mallory reaction of tertiary benzanilides promoted by visible light *via* an iminium intermediate. Experimental and theoretical analyses suggested that the iminium intermediate formed *in situ* could considerably decrease the HOMO–LUMO energy gap, resulting in visible light-induced photocyclization. A wide range of substrates, including benzoyl-substituted, aniline-substituted, *N*-substituted and heterocyclic benzanilide derivatives are compatible with this method, giving the products in good to excellent yields. In addition, this visible light-induced Mallory reaction was successfully applied to synthesize a natural alkaloid anhydrolycorinone **2v** and an AChE inhibitor *N*-methylcrinasiadine **2d**.

Data availability

All the data related to the above-mentioned manuscript are available in the ESI.†

Author contributions

D. Z., X. M. and S. W. conceived and designed the experiments and mechanism studies. D. Z. guided the project. X. M. performed DFT calculations. S. W., Z. T., J. H., T. J. and X. Z. performed the experiments. D. Z. and X. M. wrote the manuscript. All the authors discussed the results and commented on the manuscript.

Conflicts of interest

The authors declare no conflict of interest.

Acknowledgements

We are grateful for the support of this work by the National Natural Science Foundation of China (22371307, 21971267), and the program for Guangdong Introducing Innovative and Entrepreneurial Teams (2017ZT07C069). The Fundamental Research Funds for the Central Universities, Sun Yat-sen University (24qnpy058).

Notes and references

1 F. B. Mallory, C. S. Wood and J. T. Gordon, *J. Am. Chem. Soc.*, 1964, **86**, 3094–3102.
2 A. G. Lvov, *J. Org. Chem.*, 2020, **85**, 8749–8759.
3 A. Ghosh, D. Csókás, M. Budanović, R. D. Webster, I. Pápai and M. C. Stuparu, *Chem. Sci.*, 2021, **12**, 3977–3983.
4 N. Hoffmann, *Chem. Rev.*, 2008, **108**, 1052–1103.
5 T. Moriguchi, M. Higashi, D. Yakeya, V. Jalli, A. Tsuge, T. Okauchi, S. Nagamatsu and W. Takashima, *J. Mol. Struct.*, 2017, **1127**, 413–418.
6 M. K. Weclawski, M. Jakesová, M. Charyton, N. Demitri, B. Koszarna, K. Oppelt, S. Sariciftci, D. T. Gryko and E. D. Glowacki, *J. Mater. Chem. A*, 2017, **5**, 20780–20788.
7 D. Zanetti, O. Matuszewska, G. Giorgianni, C. Pezzetta, N. Demitri and D. Bonifazi, *JACS Au*, 2023, **3**, 3045–3054.
8 A. Jolly, D. Miao, M. Daigle and J. F. Morin, *Angew. Chem., Int. Ed.*, 2019, **59**, 4624–4633.
9 H. Y. Li, X. Y. Niu, S. S. Zhang, S. Shen, Q. Y. Meng and X. L. Yang, *Org. Lett.*, 2024, **26**, 5364–5369.
10 J. Bao and P. M. Weber, *J. Am. Chem. Soc.*, 2011, **133**, 4164–4167.
11 E. B. Hulley and E. L. Clennan, *J. Am. Chem. Soc.*, 2024, **146**, 1122–1131.
12 K. B. Jørgensen, *Molecules*, 2010, **15**, 4334–4358.
13 B. S. Thyagarajan, N. Kharasch, H. B. Lewis and W. Wolf, *Chem. Commun.*, 1967, 614–615.
14 N. Wang, D. Wang, Y. He, J. Xi, T. Wang, Y. Liang and Z. Zhang, *Adv. Synth. Catal.*, 2022, **364**, 1150–1155.
15 Y. Kanaoka and K. Itoh, *J. Chem. Soc., Chem. Commun.*, 1973, 647–648.
16 J. Grimshaw and A. P. d. Silva, *J. Chem. Soc., Chem. Commun.*, 1980, 302–303.
17 N. Aravindan, V. Vinayagam and M. Jeganmohan, *Org. Lett.*, 2022, **24**, 5260–5265.

18 S. K. Bera and P. Mal, *J. Org. Chem.*, 2021, **86**, 14144–14159.
19 D. Ferraris, Y. S. Ko, T. Pahutski, R. P. Ficco, L. Serdyuk, C. Alemu, C. Bradford, T. Chiou, R. Hoover, S. Huang, S. Lautar, S. Liang, Q. A. Lin, M. X. C. Lu, M. Mooney, L. Morgan, Y. Z. Qian, S. Tran, L. R. Williams, Q. Y. Wu, J. Zhang, Y. N. Zou and V. Kalish, *J. Med. Chem.*, 2003, **46**, 3138–3151.
20 T. S. Manikandan, R. Ramesh and D. Semeril, *Organometallics*, 2018, **38**, 319–328.
21 Y. Nishiyama, S. Mori, M. Makishima, S. Fujii, H. Kagechika, Y. Hashimoto and M. Ishikawa, *ACS Med. Chem. Lett.*, 2018, **9**, 641–645.
22 A. L. Ruchelman, P. J. Houghton, N. Zhou, A. Liu, L. F. Liu and E. J. LaVoie, *J. Med. Chem.*, 2005, **48**, 792–804.
23 F. Rafiee, *Appl. Organomet. Chem.*, 2017, **31**, e3820.
24 D. Bondar, O. Bragina, J. Y. Lee, I. Semenyuta, I. Järving, V. Brovarets, P. Wipf, I. Bahar and Y. Karpichev, *Helv. Chim. Acta*, 2023, **106**, e202300133.
25 M. Cohen-Armon, *Cancers*, 2020, **12**, 1628.
26 Y. Q. Wang, P. Y. Wang, Y. T. Wang, G. F. Yang, A. Zhang and Z. H. Miao, *J. Med. Chem.*, 2016, **59**, 9575–9598.
27 M. Wan, L. Zhang, Y. Chen, Q. Li, W. Fan, Q. Xue, F. Yan and W. Song, *Front. Oncol.*, 2019, **9**, 274.
28 W. E. Campbell, J. J. Nair, D. W. Gammon, C. Codina, J. Bastida, F. Viladomat, P. J. Smith and C. F. Albrecht, *Phytochemistry*, 2000, **53**, 587–591.
29 N. Conde, F. Churruca, R. SanMartin, M. T. Herrero and E. Domínguez, *Adv. Synth. Catal.*, 2015, **357**, 1525–1531.
30 M. Feng, B. Tang, H. X. Xu and X. Jiang, *Org. Lett.*, 2016, **18**, 4352–4355.
31 X. Abel-Snape, A. Whyte and M. Lautens, *Org. Lett.*, 2020, **22**, 7920–7925.
32 L. Donati, P. Leproux, E. Prost, S. Michel, F. Tillequin, V. Gandon and F. H. Porée, *Chem.–Eur. J.*, 2011, **17**, 12809–12819.
33 C. S. Nervig, P. J. Waller and D. Kalyani, *Org. Lett.*, 2012, **14**, 4838–4841.
34 X. Geng, H. He, A. Shatskiy, E. V. Stepanova, G. R. Alvey, J. Q. Liu, M. D. Kärkäs and X. S. Wang, *J. Org. Chem.*, 2023, **88**, 12738–12743.
35 Y. Fanga and G. K. Tranmer, *Med. Chem. Commun.*, 2016, **7**, 720–724.
36 K. Q. Chen, B. B. Zhang, Z. X. Wang and X. Y. Chen, *Org. Lett.*, 2022, **24**, 4598–4602.
37 C. S. Yeung, X. Zhao, N. Borduas and V. M. Dong, *Chem. Sci.*, 2010, **1**, 331–336.
38 K. Okamoto, N. Shida, H. Morizumi, Y. Kitano and K. Chiba, *Angew. Chem., Int. Ed.*, 2022, **61**, e202206064.
39 A. Itai, Y. Toriumi, N. Tomioka, H. Kagechika, I. Azumaya and K. Shudo, *Tetrahedron Lett.*, 1989, **30**, 6177–6180.
40 C. R. Kemnitz and M. J. Loewen, *J. Am. Chem. Soc.*, 2007, **129**, 2521–2528.
41 M. Szostak and J. Aubé, *Chem. Rev.*, 2013, **113**, 5701–5765.
42 K. L. White, M. Mewald and M. Movassaghi, *J. Org. Chem.*, 2015, **80**, 7403–7411.
43 H. Meier, *Angew. Chem., Int. Ed.*, 1992, **31**, 1399–1420.
44 D. Drelinkiewicz, S. T. Alston, T. Durand and R. J. Whitby, *React. Chem. Eng.*, 2023, **8**, 2134–2140.
45 B. C. Baciu, J. A. Verges and A. Guijarro, *J. Org. Chem.*, 2021, **86**, 5668–5679.
46 Z. Tang, K. Mo, X. Ma, J. Huang and D. Zhao, *Angew. Chem., Int. Ed.*, 2022, **61**, e202208089.
47 Z. Chang, J. Huang, S. Wang, G. Chen, H. Zhao, R. Wang and D. Zhao, *Nat. Commun.*, 2021, **12**, 4342.
48 J. W. Beatty and C. R. J. Stephenson, *Acc. Chem. Res.*, 2015, **48**, 1474–1484.
49 Z. Y. Cao, T. Ghosh and P. Melchiorre, *Nat. Commun.*, 2018, **9**, 3274.
50 M. Silvi, C. Verrier, Y. P. Rey, L. Buzzetti and P. Melchiorre, *Nat. Chem.*, 2017, **9**, 868–873.
51 C. R. Gonçalves, M. Lemmerer, C. J. Teskey, P. Adler, D. Kaiser, B. Maryasin, L. González and N. Maulide, *J. Am. Chem. Soc.*, 2019, **141**, 18437–18443.
52 Q. He, J. L. Ye, F. F. Xu, H. Geng, T. T. Chen, H. Chen and P. Q. Huang, *J. Org. Chem.*, 2021, **86**, 16300–16314.
53 Z. Luo, F. Wang, J. Zhang, X. Li, M. Zhang, X. Hao, Y. Xue, Y. Li, F. D. Horgen, G. Yao and Y. Zhang, *J. Nat. Prod.*, 2012, **75**, 2113–2120.
54 G. Zhan, B. Gao, J. Zhou, T. Liu, G. Zheng, Z. Jin and G. Yao, *Phytochemistry*, 2023, **207**, 113564.
55 B. Jeffries, Z. Wang, H. R. Felstead, J. Y. L. Questel, J. S. Scott, E. Chiarparin, J. Graton and B. Linclau, *J. Med. Chem.*, 2020, **63**, 1002–1031.
56 K. Martin, C. Melan, T. Cauchy and N. Avarvari, *ChemPhotoChem*, 2022, **6**, e202100215.
57 D. Hashemi, X. Ma, R. Ansari, J. Kim and J. Kieffer, *Phys. Chem. Chem. Phys.*, 2019, **21**, 789–799.
58 N. Herrero-García, I. Fernández and J. O. Barcina, *Chem.–Eur. J.*, 2011, **17**, 7327–7335.
59 T. Lu and F. Chen, *J. Comput. Chem.*, 2011, **33**, 580–592.
60 Z. Liu, T. Lu and Q. Chen, *Carbon*, 2020, **165**, 461–467.
61 G.-J. Huang, M. A. Harris, M. D. Krzyaniak, E. A. Margulies, S. M. Dyar, R. J. Lindquist, Y. Wu, V. V. Roznyatovskiy, Y.-L. Wu, R. M. Young and M. R. Wasielewski, *J. Phys. Chem. B*, 2016, **120**, 756–765.
62 N. A. Garcia and T. Kowalczyk, *J. Phys. Chem. C*, 2017, **121**, 20673–20679.
63 X. Zhang, X. Chen and J. Zhao, *Dalton Trans.*, 2021, **50**, 59–67.
64 J. L. Garnett, M. L. Long and R. F. W. Vining, *J. Am. Chem. Soc.*, 1972, **94**, 5914–5915.
65 Y. P. Liu, C. J. Zhu, C. C. Yu, A. E. Wang and P. Q. Huang, *Eur. J. Org Chem.*, 2019, 7169–7174.
66 J. J. Murphy, D. Bastida, S. Paria, M. Fagnoni and P. Melchiorre, *Nature*, 2016, **532**, 218–222.
67 J. J. Zhao, H. H. Zhang, X. Shen and S. Yu, *Org. Lett.*, 2019, **21**, 913–916.
68 B. A. Jones, P. Solon, M. V. Popescu, J. Y. Du, R. Paton and M. D. Smith, *J. Am. Chem. Soc.*, 2023, **145**, 171–178.
69 Y. G. Shi, S. K. Mellerup, K. Yuan, G. F. Hu, F. Sauriol, T. Peng, N. Wang, P. Chen and S. Wang, *Chem. Sci.*, 2018, **9**, 3844–3855.